Experimental Study of Spectrum Sensing based on Energy Detection and Network Cooperation

Danijela Cabric	Artem Tkachenko	Robert W. Brodersen
Berkeley Wireless Research Center	Berkeley Wireless Research Center	Berkeley Wireless Research Center
2108 Allston Way #200	2108 Allston Way #200	2108 Allston Way #200
Berkeley, CA 94704	Berkeley, CA 94704	Berkeley, CA 94704
++ 1-510-666-3192	++ 1-510-666-3100	++ 1-510-666-3110
danijela@eecs.berkeley.edu	artemtk@eecs.berkeley.edu	rb@eecs.berkeley.edu

ABSTRACT

Spectrum sensing has been identified as a key enabling functionality to ensure that cognitive radios would not interfere with primary users, by reliably detecting primary user signals. Recent research studied spectrum sensing using energy detection and network cooperation via modeling and simulations. However, there is a lack of experimental study that shows the feasibility and practical performance limits of this approach under real noise and interference sources in wireless channels. In this work, we implemented energy detector on a wireless testbed and measured the required sensing time needed to achieve the desired probability of detection and false alarm for modulated and sinewave-pilot signals in low SNR regime. We measured the minimum detectable signal levels set by the receiver noise uncertainties. Our experimental study also measured the sensing improvements achieved via network cooperation, identified the robust threshold rule for hard decision combining and quantified the effects of spatial separation between radios in indoor environments.

1. INTRODUCTION

Recently, Cognitive Radios (CRs) have been proposed as a possible solution to improve spectrum utilization via opportunistic spectrum sharing. Cognitive radios are considered lower priority or secondary users of spectrum allocated to a primary user. Their fundamental requirement is to avoid interference to potential primary users in their vicinity. Spectrum sensing has been identified as a key enabling functionality to ensure that cognitive radios would not interfere with primary users, by reliably detecting primary user signals. In addition, reliable sensing creates spectrum opportunities for capacity increase of cognitive networks.

The first application of spectrum sensing is studied under IEEE 802.22 standard group [1] in order to enable secondary use of UHF spectrum for a fixed wireless access. In addition, there is a number of indoor applications where spectrum sensing would increase spectrum efficiency and utilization. For example, it could improve co-existence of WLANs (802.11) [2], or create new spectrum opportunities for sensor and ad-hoc networks [3]. Regardless of application, sensing requirements are based on primary user modulation type, power, frequency and temporal parameters. For example, the actual primary signal used for sensing could be the regular data transmission signal.

Alternatively, it could be a special permission or denial signal to use the spectrum, in the form of a pilot or a beacon.

Spectrum sensing is often considered as a detection problem, which has been extensively researched since early days of radar [4]. However, the key challenge of spectrum sensing is the detection of weak signals in noise with a very small probability of miss detection, which requires better understanding of very low SNR regimes [5]. In addition, spectrum sensing is a cross-layer design problem in the context of communication networks. Cognitive radio sensing performance can be improved by enhancing radio RF front-end sensitivity, exploiting digital signal processing gain, and using network cooperation where users share their spectrum sensing measurements [6].

Our goal is to provide a comprehensive study, supported with experimental data, that addresses the following issues in spectrum sensing based on energy detection:

-Required sensing time needed to achieve the desired probability of detection and false alarm.

-Limitations of the energy detector performance due to presence of noise uncertainty and background interference.

-Performance improvements offered by network cooperation. How does the performance scale with the number of radios? What is the robust threshold rule? What is the effect of spatial separation between cooperating radios?

The paper is organized as follows: Section 2 reviews the energy detector model, derives its performance and addresses the limitations. In section 3, we provide the experimental data that verifies theoretical results and characterizes energy detector performance in noise. In section 4, we discuss the cooperation gains in fading channels. Section 5 presents the experimental data for cooperation. Summary of the work and conclusions are presented in Section 6.

2. ENERGY DETECTION CHARACTERIZATION

2.1 Model

We consider the detection of a weak deterministic signal in additive noise. The signal power is confined inside *a priori* known bandwidth B around central frequency f_c (Figure 1). We assume that activity outside of this band is unknown. Two
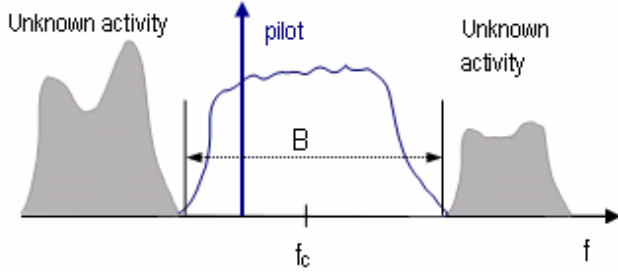
Figure 1. Spectrum Picture

deterministic types of signal are considered: sinewave tone (pilot) and modulated signal with unknown data.

An optimal detector based on matched filter is not an option since it would require the knowledge of the data for coherent processing. Instead a suboptimal energy detector is adopted, which can be applied to any signal type. Conventional energy detector consists of a low pass filter to reject out of band noise and adjacent signals, Nyquist sampling A/D converter, square-law device and integrator (Figure 2.a).

Without loss of generality, we can consider a complex baseband equivalent of the energy detector. The detection is the test of the following two hypotheses:

H_0: $Y[n] = W[n]$ signal absent
H_1: $Y[n] = X[n] + W[n]$ signal present
$n = 1,..., N$; where N is observation interval   (1)

The noise is assumed to be additive, white and Gaussian (AWGN) with zero mean and variance σ_w^2. In the absence of coherent detection, the signal samples can also be modeled as Gaussian random process with variance σ_x^2. Note that over-sampling would correlate noise samples and, in principle, the model could be always reduced to (1).

A decision statistic for energy detector is:

$$T = \sum_N (Y[n])^2 \qquad (2)$$

Note that for a given signal bandwidth B, a pre-filter matched to the bandwidth of the signal needs to be applied. This implementation is quite inflexible, particularly in the case of narrowband signals and sinewaves. An alternative approach could be devised by using a periodogram to estimate the spectrum via squared magnitude of the FFT, as depicted in Figure 2.b). This
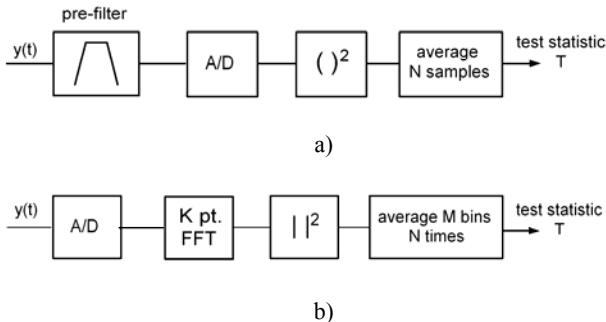

a)

b)

Figure 2. a) Implementation with analog pre-filter and square-law device   b) implementation using periodogram: FFT magnitude squared and averaging

architecture also provides the flexibility to process wider bandwidths and sense multiple signals simultaneously. As a consequence, an arbitrary bandwidth of the modulated signal could be processed by selecting corresponding frequency bins in the periodogram.

In this architecture, we have two degrees of freedom to improve the signal detection. The frequency resolution of the FFT increases with the number of points K (equivalent to changing the analog pre-filter), which effectively increases the sensing time. In addition, increasing the number of averages N also improves the estimate of the signal energy. In practice, it is common to choose a fixed FFT size to meet the desired resolution with a moderate complexity and low latency. Then, the number of spectral averages becomes the parameter used to meet the detector performance goal. We consider this approach in our experiments.

2.2 Performance

It is well known that under the common detection performance criteria (most notably, the Neyman-Pearson criteria) likelihood ratio yields the optimal hypothesis testing solution and performance is measured by a resulting pair of detection and false alarm probabilities (P_d, P_{fa}). Each pair is associated with the particular threshold γ that tests the decision statistic:

$T > \gamma$ *decide signal present*
$T < \gamma$ *decide signal absent*

When the signal is absent, the decision statistic has a central chi-square distribution with N degrees of freedom. When the signal is present, the decision statistic has a non-central chi-square distribution with the same number of degrees of freedom. Since we are interested in the low SNR regime, the number of required samples is large. If $N > 250$ we can use the central limit theorem to approximate the test statistic as Gaussian.

$T \sim Normal(N\sigma_w^2, 2N\sigma_w^4)$ under H_0
$T \sim Normal(N(\sigma_w^2 + \sigma_x^2), 2N(\sigma_w^2 + \sigma_x^2)^2)$ under H_1

Then P_d and P_{fa} can be evaluated as:

$$P_{fa} = Q(\frac{\gamma - N\sigma_w^2}{\sqrt{2N\sigma_w^4}}) \quad P_d = Q(\frac{\gamma - N(\sigma_w^2 + \sigma_x^2)}{\sqrt{2N(\sigma_w^2 + \sigma_x^2)^2}}) \quad (3)$$

Note that for the constant false alarm probability (CFAR), the threshold γ can be set even without the knowledge of the signal power. Then, for the fixed number of samples N, P_d can be evaluated by substituting the threshold in (3). Each threshold corresponds to a pair (P_{fa}, P_d), representing the receiver operating curve (ROC).

If the number of samples used in sensing is not limited, an energy detector can meet any desired P_d and P_{fa} simultaneously. The minimum number of samples is a function of the signal to noise ratio $SNR = \sigma_x^2 / \sigma_w^2$:

$$N = 2[(Q^{-1}(P_{fa}) - Q^{-1}(P_d))SNR^{-1} - Q^{-1}(P_d)]^2 \qquad (4)$$

In the low $SNR << 1$ regime, number of samples required for the detection, that meets specified P_d and P_{fa}, scales as $O(1/SNR^2)$. This inverse quadratic scaling is significantly inferior to the optimum matched filter detector whose sensing time scales as

O(1/SNR) [5]. The exception is the sinewave case, where the optimum matched filter is the FFT with length equal to the multiple of sinewave period. If the FFT length is not matched, then spectral leakage occurs. Therefore, the implementation in Figure 2.b) is partially coherent for sinewave sensing, and it is expected that its sensing time scales better than $O(1/SNR^2)$.

2.3 Limitations

Unfortunately, an increased sensing time is not the only disadvantage of the energy detector. More importantly, there is a minimum SNR below which signal cannot be detected, and when the formula (4) no longer holds. This minimum SNR level is referred to SNR_{wall} [7]. In order to understand when the detection becomes impossible we need to revisit our signal model. There, we have made two very strong assumptions (that are typically made in communications system analysis). First, we assumed that noise is white, additive and Gaussian, with zero mean and known variance. However, noise is an aggregation of various sources including not only thermal noise at the receiver and underlined circuits, but also interference due to nearby unintended emissions, weak signals from transmitters very far away, etc. Second, we assumed that noise variance is precisely known to the receiver, so that the threshold can be set accordingly. However, this is practically impossible as noise could vary over time due to temperature change, ambient interference, filtering, etc. Even if the receiver estimates it, there is a resulting estimation error due to limited amount of time. Therefore, our model needs to incorporate the measure of noise variance uncertainty.

How does the noise uncertainty affect detection of signals in low SNR? Essentially, setting the threshold too high based on the wrong noise variance, would never allow the signal to be detected. If there is a x dB noise uncertainty, then the detection is impossible below $SNR_{wall}=10\log_{10}[10^{(x/10)}-1]$dB [7]. For example, if there is a 0.5 dB uncertainty in the noise variance, then signal in -21dB SNR cannot be detected using energy detector.

3. ENERGY DETECTOR EXPERIMENTAL RESULTS

The goal of our experimental study was to evaluate and verify the theoretical results on the performance and limitations of the energy detector. In particular, we measured the achievable probabilities of detection as a function of sensing time, and the existence and position of the SNR_{wall}. The need for experiments is stressed by the inability to realistically model all noise source encountered in the receiver and interference environment. In addition, a comprehensive evaluation of P_d and P_{fa} requires extensive Monte Carlo simulations. Therefore, the implementation on a real-time testbed allows us to perform a large set of experiments for various signal levels and receiver settings. We also provide an example of hardware implementation with report on computational complexity, area, and speed. To the best of our knowledge, this is the first energy detector study that incorporates hardware realization and real-time experiments.

3.1 Testbed Description

The testbed used in the experiments [8] is built around the

Berkeley Emulation Engine 2 (BEE2), a generic multi-purpose FPGA based, emulation platform for computationally intensive applications. The BEE2 consists of 5 Vertex-IIPro70 FPGAs, 1 for control and 4 for user applications. Control FPGA runs Linux and a full IP protocol stack convenient for connection with laptops and other network devices. Linux OS has been enhanced to allow access to hardware registers and memory on the user FPGA for real-time data access and control. We used BWRC-developed automation tool to map our signal processing algorithms design in Xilinx System Generator library to FPGA configurations.

BEE2 can connect up to 18 front-end boards via 10 Gbit/s full duplex Infiniband interfaces. By using optical transceivers compatible with Infiniband connectors, optical cable can connect front-end boards at distances up to 1/3 of a mile away from BEE2 in order to perform different scenario experiments and implement network cooperation. In addition, the optical link provides good analog signal isolation on the front-end side from the digital noise sources created by BEE2.

The radio front-end system operates in 2.4 GHz ISM band over 85 MHz of bandwidth with programmable center frequency and several gain control stages. Antennas used in the experiments are single monopole rubberduck with 0 dBi omnidirectional pattern at 2.4 GHz. The analog/baseband board contains a 14-bit 128 MHz D/A converters, 12-bit 64 MHz A/D converters, and 32 MHz wide baseband filters. On board Virtex-IIPro20 is used to implement radio control functions and provide optical transceiver interface to BEE2 for sample processing.

For the transmitter, we used Agilent EE4438C ESG vector signal generator. It is calibrated to output absolute signal levels for arbitrary signals and modulation types. The transmitter was interfaced to BEE2 via 100 Base-T Ethernet so that signal parameters can be changed during the runtime of the experiments. The test setup is presented in Figure 3.

3.2 Energy Detection Implementation

The energy detector is implemented using 1024 point FFT with a fully parallel pipelined architecture for the fastest speed. Due to A/D sampling at 64 MHz, this implementation has 62.5 kHz FFT bin resolution. Each block of FFT outputs is averaged using an accumulator with programmable number of averages. The result of the computation is stored in the memory block RAM. The
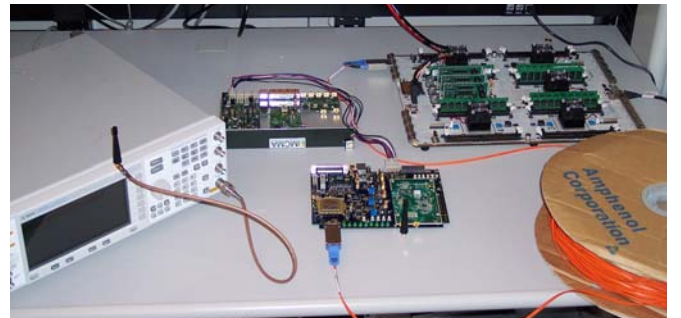

Figure 3. Testbed: Signal generator, Radio board, BEE2 and optical cable

software running on the BEE2 control FPGA sets all sensing parameters and then loads the processed data from the block RAMs. The design runs at 100 MHz speed, while the signal samples from the radio are fed at 64MHz. Thus, there is an insignificant latency in the signal processing. For example, executing 1000 experiments with 3200 spectral averages (51.2 ms) of 1024 FFT takes less than 60 seconds. Hardware estimate of this design is: 15,416 FPGA logic slices, 140 18x18 multipliers, and 106 block RAMs.

3.3 Experimental Setup

To measure the performance under AWGN we connect signal generator to the RF board antenna input via SMA cable. The radio is put inside the RF shield, thus the only noise sources come from the radio circuitry. Prior to all experiments, we calibrated the noise level of the radio receiver, and the measured level is -103 dBm in a 62.5 kHz FFT bin. In order to accommodate a wide dynamic range signal and keep A/D resolution high, we set the total receiver gain to medium level of 50dB.

We tested two types of signals: sinewave carrier at 2.493GHz,

a) Sinewave sensing

b) QPSK sensing

Figure 4. Probability of detection vs. sensing time for P_{fa}=5%

and 4 MHz wide QPSK signal centered at the same carrier. For sinewave carrier we swept signal levels from -110 dBm to -128 dBm, which is equivalent to -7 to -25 dB of the receiver *SNR*. For 4 MHz QPSK signal, we tested levels from -98 dBm to -110 dBm, which is equivalent to -13 to -25 dB of the receiver *SNR*. In order to accurately estimate the P_d and P_{fa} we repeated each detection measurement 1000 times. For each signal level, we collected two sets of energy detector outputs: one in the presence, and the other in the absence of the signal generator output signal. From "no input signal" data, we estimated the detection threshold to meet the specified probability of false alarm. Then, we applied the threshold to the data where signal was present and computed the probability of detection.

3.4 Results

First, we measure how the probability of detection scales as the sensing time increases. For all measurements, we set the probability of false alarm to 5%. Figure 4.a) shows the achievable probabilities of detection for sinewave carrier when number of averages increases from 200 (3.2 ms) to 52,000 (0.83 s). If we set the P_d to a reasonable limit of 0.8 then within 200 ms energy detector can detect up to -122 dBm. Figure 4.b) shows the performance of the detector for the QPSK signal. Since the energy of the QPSK signal is spread over a wider bandwidth, it becomes harder to detect weak signals in additive noise. The target P_d=0.8 can be achieved for signals greater than -104 dBm within 170 ms.

Figure 4 also shows that when the signal becomes too weak, increasing the number of averages does not improve the detection. This result is expected and is explained by the SNR$_{wall}$ existence. In Figure 5, we plot the required sensing time vs. input signal levels in order to meet P_d and P_{fa} requirements simultaneously. We set the P_{fa}=0.05 and P_d=0.6. In the case of sinewave sensing we observe the scaling law $N \sim 1/SNR^{1.5}$.This is expected since our implementation has a partial coherent processing gain for sinewave detection. However, beyond -124 dBm signal level the slope becomes increasingly steep. Signals below -128 dBm cannot be detected, resulting in the SNR$_{wall}$=-25dB. In the case of QPSK detection, we observe a non-coherent detection scaling law of $N \sim 1/SNR^2$ consistent with the theoretical prediction. The limit in QPSK detection happens at -110dBm (SNR$_{wall}$=-25dBm). From the theoretical analysis, we know that SNR$_{wall}$=-25dB corresponds to less than 0.5 dB of noise uncertainty.

4. COOPERATIVE SENSING

Up to this point we have considered spectrum sensing performed by a single radio in AWGN-like channels. In fading channels, however, single radio sensing requirements are set by the worst case channel conditions introduced by multipath, shadowing and local interference. These conditions could easily result in SNR regimes below the SNR$_{wall}$, where the detection will not be possible. However, due to variability of signal strength at various locations, this worst case condition could be avoided if multiple radios share their individual sensing measurements via network cooperation [9],[10],[11].
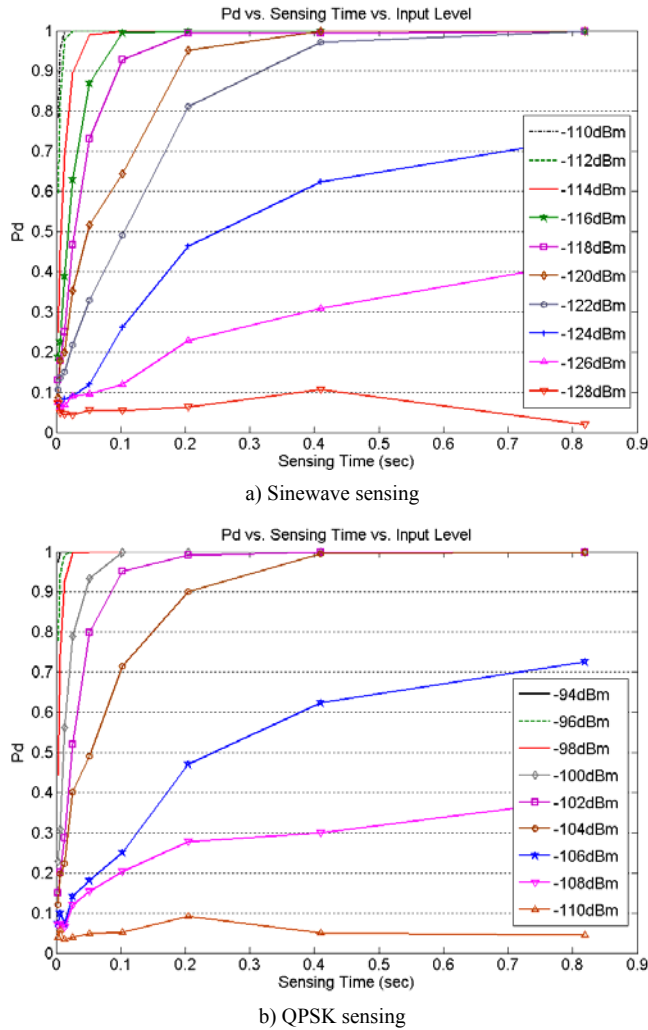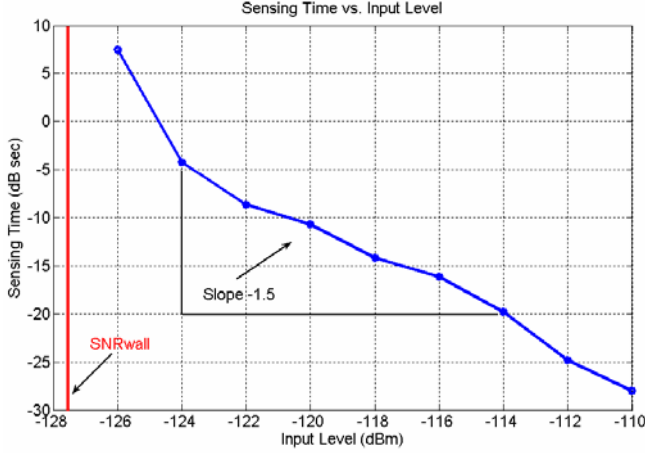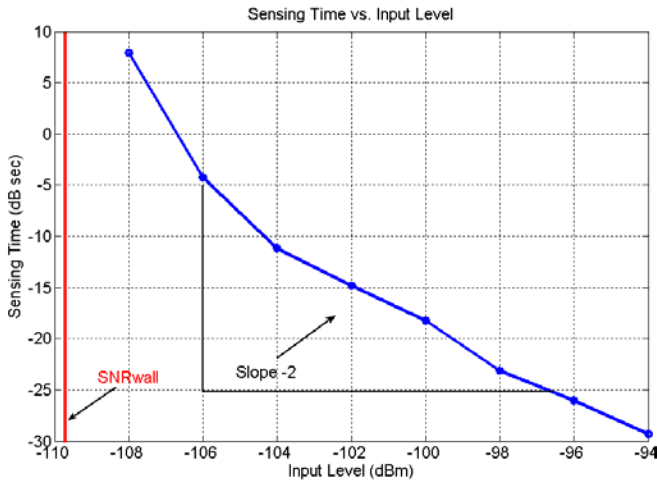
a) Sinewave sensing

b) QPSK sensing

Figure 5. Required sensing time vs. signal input level for fixed P_d and P_{fa}

4.1 Cooperation Gains

Under independent fading conditions, which is often assumed for multipath if radios are more than $\lambda/2$ apart, cooperation can be studied as a diversity gain in multiple antenna channels. Due to a small overhead in the protocol, we consider a hard decision combining, where each radio sends its local decision to a centralized location (0 signal is absent, 1 signal is present), and the decisions is made via OR operation. It has been shown [9] that if n radios combine independent measurements, then probability of detection of the system Q_D monotonically increases as $Q_D=1-(1-P_d)^n$. In addition, the probability of false alarm for the system Q_F also monotonically increases as $Q_F=1-(1-P_{fa})^n$.

However, fading could be caused by shadowing that exhibits high correlation if two radios are blocked by the same obstacle. Commonly, a shadowing correlation is described by the coefficient ρ and modeled as an exponential function of distance: $\rho=e^{-ad}$. Measurements of the shadowing in indoor environments

[12] show that the correlation coefficient is independent of wavelength over a frequency octave, but it is dependent on the topography. It was estimated [12] that 90% correlation distance is typically 1m, 50 % is around 2m, and slowly decays to 30% over 8m. Therefore, in the limited area, increasing the number of radios introduces the correlation, which in effect limits the cooperation gain [9], [11]. In our experimental study, we investigate how the cooperation gain scales with the number of radios and their spatial separation in typical indoor environments.

4.2 Threshold Rules

Recall the single radio analysis where we identified the SNR_{wall} due to noise uncertainty and its impact on the detection threshold. Now, in the cooperation case, radios could use two different types of threshold rules in the local decision process: 1) a predetermined (fixed) threshold set by the centralized processor or 2) an independently estimated threshold based on the local noise and interference measurements. In the case of stationary environments with all radios being identical, these two rules would result in the same system performance. However, due to the presence of ambient interference caused by primary or cognitive radios in the vicinity, and local noise, temperature, and circuit variability, each radio sees different aggregate noise and interference. This observation suggests that a fixed threshold might be suboptimal, and that in practical situations the estimated threshold would provide robustness and better gains. Through experiments, we analyze benefits of noise and interference estimation, and the gap between the two threshold rules.

5. EXPERIMENTAL RESULTS FOR COOPERATION

5.1 Experimental Setup

The experiments were conducted inside the Berkeley Wireless Research Center. The floor plan of the center is shown in Figure 6. The figure also shows 54 locations on a 2m by 2m grid, that covers a cubicle area, library and conference room, where all wireless measurements were taken. In all experiments, the

Figure 6. BWRC floor plan with transmitter and receiver locations

transmitter was located inside the lab. Therefore, the signal path between the transmitter and all receiver positions included propagation through either concrete or wooden walls, supporting beams, medium and large size metal cabinets, and general office furniture. The area covers a balanced variation of obstacles which are typical for indoor non-line-of-sight environments.

Due to operation in the unlicensed ISM band, outside interference had to be considered. All 802.11 b/g, Bluetooth, and ZigBee equipment was shut down during the experimentation, in order to minimize potential interference. For the sinewave, the signal generator transmitted a -40 dBm signal at 2.485GHz. For the 4 MHz wide QPSK signal, the signal generator transmitted a -30 dBm signal in 2.483GHz – 2.487GHz band, centered at 2.485GHz. The bandwidth ratio of QPSK signal to sinewave is approximately $10*1\log_{10}$(4 MHz/62.5kHz)=18 dB, thus a 10 dB difference in transmit power favors the sinewave case in terms of the receiver SNR. It was expected that sinewave performance would be more affected by multipath, thus 8 dB power gain was

added.

For each sensing location, data was collected for three different transmitter configurations: idle spectrum i.e. no signal, sinewave signal and QPSK signal. The idle spectrum was sensed in order to be able to compare two different threshold rules described in the previous sections. For each location and data type, spectrum was sensed 200 consecutive times using 3200 averages (51.2 ms) in the periodogram.

5.2 Measurement Results

First, we analyze the cooperation gain as function of the number of cooperating radios. Figures 7 a) and b) show the system ROCs for sinewave and wideband QPSK signals, respectively. For a given probability of false alarm for the cooperating system Q_F, an estimated threshold was computed for each location based on the idle spectrum data. Then, these thresholds were used to compute the probability of detection for each location. By applying the OR function to decisions of n radios and averaging across all possible combination of n radios among 54 locations, we obtain Q_D.

For the sinewave signal, the single radio sensing is limited by multipath fading, thus significant improvement is achieved even with 2 cooperative radios. Given 10% probability of false alarm, an 18% improvement is observed through cooperation of two radios, then 9% for three, and it saturates to 4% and 3% for four and five cooperating radios, respectively. Overall, going from 1 to 5 cooperative radios detection improves from 63% to 97%. Note that if radios would experience the independent multipaths then the cooperation would result in Q_D=1-(1-0.63)[5]=99%. In the case of wideband QPSK signal, the probability of detection is even better, though the average SNR is 8dB lower. With 5 cooperative radios, Q_D for QPSK reaches 99%. This improvement in the QPSK sensing is due to frequency diversity gain, which makes the wideband signal less sensitive to deep fades.

Next, we compare experimental results for two different threshold rules applied to the same set of measurement data. For the fixed threshold rule, the same threshold is applied for all possible combinations of cooperating radios. As expected, Figure 8 shows

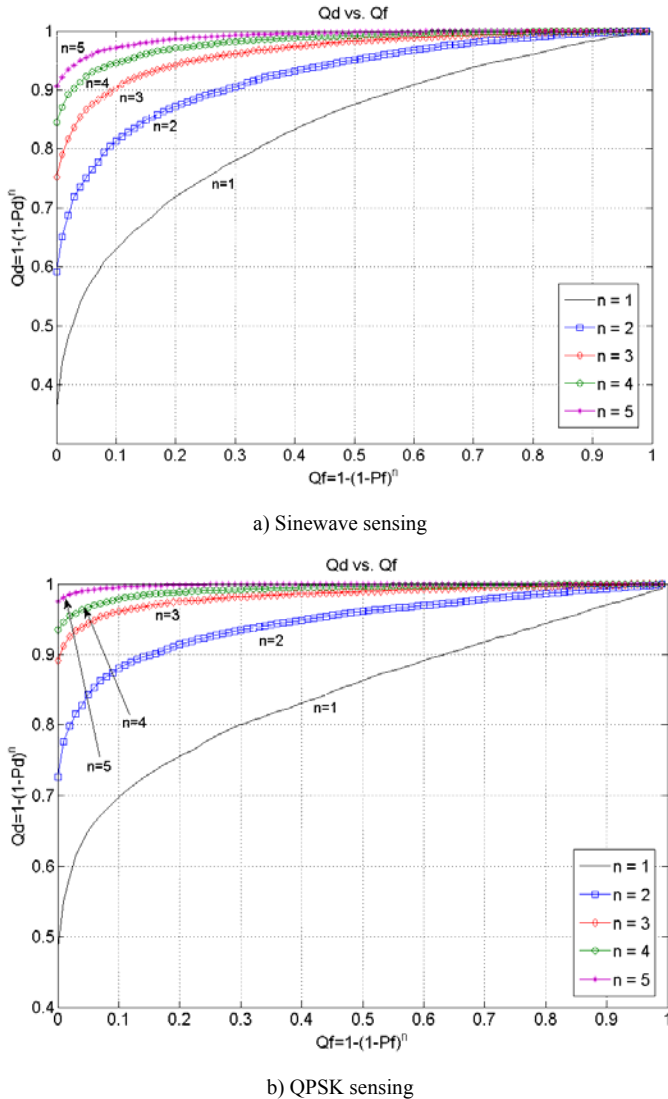a) Sinewave sensing

b) QPSK sensing

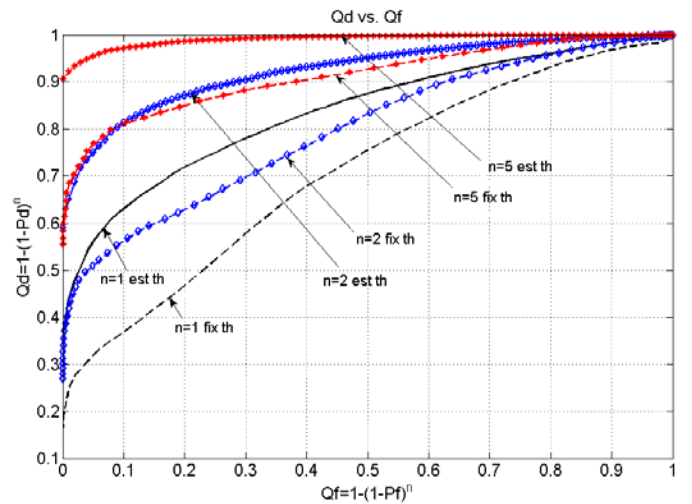Figure 7. Cooperative gains vs. number of cooperative radios

Figure 8. Cooperative gains vs. threshold rule

that the performance of the fixed threshold rule is significantly lower than that of the estimated threshold rule. Even for the single radio sensing under variable noise and interference, it is essential to apply the location and time relevant threshold obtained via estimation. The cooperation gains are still present, but are significantly reduced by suboptimal threshold rule. The gap between the two rules varies form 15% to 25%. Thus, even a moderate Q_D=90 % and Q_F=10% can never be met using the fixed threshold. The implications of this result imply that robust sensing must involve frequent receiver noise calibration and accurate interference estimation. In turn, this might require additional sensing time.

Lastly, we analyze the effect of spatial correlation on the probability of detection for two cooperating radios. Figure 9 presents experimental results for sinewave and 4 MHz QPSK signals for separation distances from 2 m to 8 m. Measurements show that the probability of detection monotonically increases as the separation between two cooperating radios increases. The improvement of up to 7% in Q_D is obtained once the cooperation distances extend to 8 m. This result can be explained by measurements in [12] showing that correlation coefficient of 50% for distances of 2 m is still high to provide independency needed for cooperation gain. In [9], simulation study has shown that cooperation gain increases Q_D by 2-3% as the correlation coefficient drops from 50% to 10%. Our measurements confirm that it is beneficial to increase the radio separation so that correlation coefficient is less than 10%, which for this particular environment happens at 8 m distances.

6. CONCLUSIONS

In this paper we investigated the feasibility and performance of the energy detector for the spectrum sensing of narrowband pilots and wideband primary user signals. Our study includes a theoretical background and experimental results for two applications: 1) single radio sensing performed on the physical layer and 2) cooperative sensing performed by a network of cognitive radios in an indoor environment. We derived and measured the required sensing time, achievable probability of detections and false alarm, and minimum detectable signal levels in AWGN and fading channels. Experiments are performed in the 2.4 GHz ISM band using a radio testbed whose front-end and baseband circuitry exhibit true noise, gain and filtering variability. In AWGN-like channels, it was found that the presence of radio uncertainties sets practical limits on minimum detectable signal levels which cannot be further improved by signal processing.

In fading channels, single radio sensing is limited by the worst case channel conditions introduced by multipath and shadowing. We deployed multiple radios in a typical office indoor environment and measured sensing improvements achieved via cooperation. Our cooperation study also identified the robust threshold rule for hard decision combining. In addition, we quantified the effects of spatial separation between cooperating radios in the typical indoor environments.
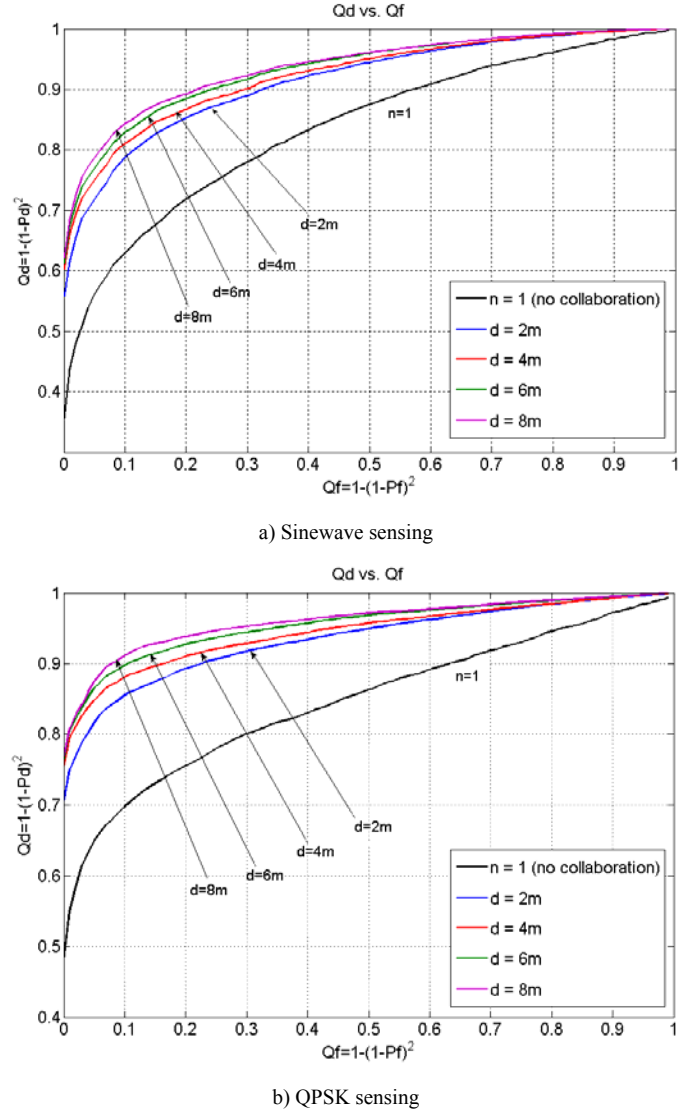

a) Sinewave sensing

b) QPSK sensing

Figure 9. Cooperation gains vs. spatial separation

7. ACKNOWLEDGMENTS

8. REFERENCES

[1] C. Cordeiro, K. Challapali, K. Birru, S. Shankar, "IEEE 802.22: the first worldwide wireless standard based on cognitive radios", In proc. of DySPAN'05, November 2005.

[2] D. Cabric, S.M. Mishra, D. Willkomm, R.W. Brodersen, A. Wolisz, "A Cognitive Radio Approach for Usage of Virtual Unlicensed Spectrum", 14th IST Mobile and Wireless Communications Summit, June 2005.

[3] B. Wild, K. Ramchandran, "Detecting Primary Receivers for Cognitive Radio Applications", In proc. of DySPAN'05, November 2005.

[4] H.Urkowitz,"Energy Detection of Unknown Deterministic Signal", In proc. of the IEEE, April 1967.

[5] A.Sahai, N.Hoven, R. Tandra. "Some Fundamental Limits on Cognitive Radio", In Allerton Conference on Communications, Control and Computing, October 2004.

[6] D.Cabric. S.M. Mishra. R.W. Brodersen, "Implementation Issues in Spectrum Sensing", In Asilomar Conference on Signal, Systems and Computers, November 2004.

[7] R. Tandra, A. Sahai. "Fundamental Limits on Detection in Low SNR", In proc. of the WirelessComm05 Symposium on Signal Processing, June 2005.

[8] S.M.Mishra, D. Cabric, C. Chang, D. Willkomm, B. van Schewick, A. Wolisz, R. Brodersen, "A Real Time Cognitive Radio Testbed for Physical and Link Layer Experiments" In proc. of DySPAN'05, November 2005

[9] A. Ghasemi, E. S. Sousa, "Collaborative Spectrum Sensing for Opportunistic Access in Fading Environments", In proc. of DySPAN'05, November 2005.

[10] E. Visotsky, S. Kuffner, R. Peterson. "On Collaborative Detection of TV Transmissions in Support of Dynamic Spectrum Sharing", In proc. of DySPAN'05, November 2005.

[11] S.M.Mishra, A.Sahai, R.W.Brodersen,"Cooperative Sensing among Cognitive Radios", In proc. of International Conference on Communications, ICC'06, June 2006.

[12] J.C. Liberti, T.S. Rappaport, "Statistics of shadowing in indoor radio channels at 900 and 1900 MHz", In proc. of Military Communications Conference, MILCOM'92, October 1992.